Dyes and Pigments 94 (2012) 224–232

Contents lists available at SciVerse ScienceDirect

Dyes and Pigments

journal homepage: www.elsevier.com/locate/dyepig

New 2,6-modified BODIPY sensitizers for dye-sensitized solar cells

Mao Mao [a], Jian-Bo Wang [a], Zu-Feng Xiao [a], Song-Yuan Dai [b], Qin-Hua Song [a,*]

[a] Department of Chemistry, University of Science and Technology of China, Hefei 230026, PR China
[b] Key Laboratory of Novel Thin Film Solar Cells, Institute of Plasma Physics, Chinese Academy of Sciences, Hefei 230031, PR China

ARTICLE INFO

Article history:
Received 1 October 2011
Received in revised form
11 January 2012
Accepted 15 January 2012
Available online 24 January 2012

Keywords:
Dye-sensitized solar cells
BODIPY
Sensitizers
Charge transfer
Structure–property relationship
Photochemistry

ABSTRACT

A series of new metal-free organic dyes with either a boron dipyrromethene (BODIPY)-phenylene or -thiophene as a π-conjugated bridge have been synthesized for application in dye-sensitized solar cells. The photophysical and electrochemical properties of these dyes were investigated and their performance as sensitizers in dye-sensitized solar cells has been measured. The structure–property relationship shows that the introduction of a methoxy group as the donor and a BODIPY-thiophene unit as the π-conjugated bridge are favorable to improve the efficiency of DSSCs. A combination of a methoxy modified donor and BODIPY-thiophene bridge possesses a stronger electron-donating ability and longer wavelength absorption band, and as a sensitizer reveals the best properties of DSSCs, whose conversion efficiency was 2.26%.

1. Introduction

Dye-sensitized solar cells (DSSCs) have attracted considerable scientific and industrial interest as promising candidates for new renewable energy sources during the past decades [1–4]. DSSCs based on Ru (II)-polypyridyl complexes photosensitizers, such as N3, N719, and the black dye (Fig. 1), have achieved remarkable light-to-power conversion efficiency above 10% under simulated sunlight (AM 1.5) illumination [5–7]. Meanwhile, metal-free organic dyes, featuring high extinction coefficients, facile molecular design, simple synthesis process, lower cost and environmentally friendliness in comparison to Ru (II) complexes, are also under investigation. Many organic dyes based on donor–(π-spacer)–acceptor system, including porphyrin [8–12], perylene [13–15], phthalocyanine [16], triarylamine [17–20], cyanine [21,22], coumarin [23–27], hemicyaine [28,29], indoline [30–32], tetrahydroquinoline [33,34] and phenothiazine [35] have been investigated as sensitizers for DSSCs.

Boron dipyrromethene (BODIPY) is an interesting fluorophore with a strong absorption coefficient in the visible and near-IR ranges, large fluorescence quantum yield, a relatively long excited-state lifetime and good solubility in organic solvents. Over the past few years BODIPY dyes have attracted considerable attention in a variety of potential applications such as biomolecule labeling and fluorescence imaging [36–41]. BODIPY dyes are also promising to be useful in DSSCs as photosensitizers [12,42–50]. In most cases, the BODIPYs were functionalized with strong donor groups at the 3- and 5-positions and a phenyl modified cyanoacrylic acid moiety at the 8-position. However, the acceptor at the 8-position bearing a phenyl group is very likely to limit conjugation and reduce electron flow from the donor to the anchor group, because the meso-phenyl group and the BODIPY core with two protruding methyl group at potions 1 and 7 are almost orthogonal [43]. DSSCs with the above dyes gave only moderate cell parameters and a maximal efficiency of 2.46% [49]. Recently it was found that the bridging groups carrying lateral alkyl chains helped to form a blocking layer to keep I_3^- ions away from the TiO_2 electrode surface, so increasing the electron lifetime and open-circuit voltage (V_{oc}). For this reason, 8-alkyl chain-substituted BODIPYs have been used as conjugated bridges, linking the donor and acceptor from 2- and 6-positions to form the D–π–A systems, which reveals high conversion efficiencies, up to 1.83% [50].

In this work, we have synthesized a series of new metal-free organic sensitizers with a 1*H*-phenanthro[9,10-*d*]imidazole moiety as the donor, BODIPY as the conjugated bridge, and a cyanoacrylic acid acting as the anchoring group (**PB1**–**4**), shown in Chart 1. The four new sensitizers have been applied to nanocrystalline TiO_2-based solar cells, and reveal better photovoltaic properties.

* Corresponding author. Fax: +86 551 3601592.
E-mail address: qhsong@ustc.edu.cn (Q.-H. Song).

0143-7208/$ – see front matter © 2012 Elsevier Ltd. All rights reserved.
doi:10.1016/j.dyepig.2012.01.011

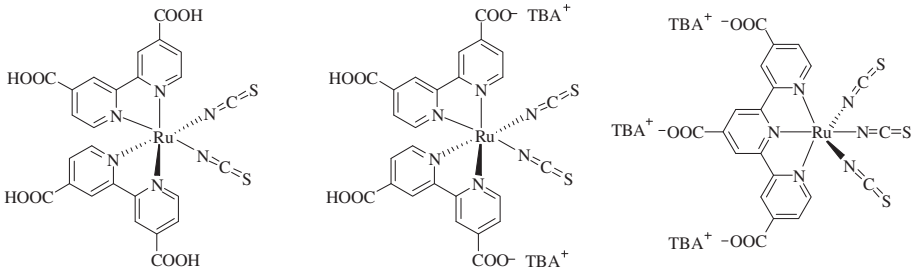

Fig. 1. The structures of **N3**, **N719** and Black dye.

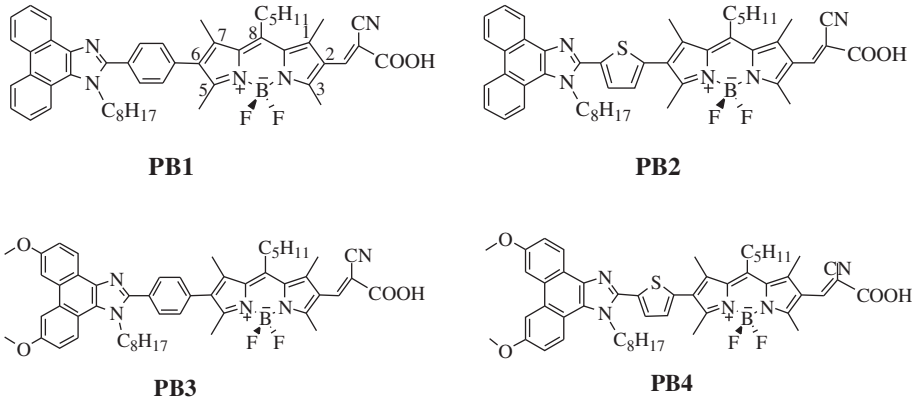

Chart 1. Molecular structures of BODIPY dyes.

2. Experimental

2.1. Reagents and instruments

Solvents for organic synthesis were reagent grade, and were dried prior to use, and solvents for measurements of spectroscopy are HPLC grade and used without further purification. All chemicals were purchased from commercial sources and used as received. NMR spectra were recorded on a Bruker AV300 spectrometer (300 MHz for ^{1}H NMR, 75 MHz for ^{13}C NMR). Mass spectra were measured on a Micromass GCT TOF and Thermo LTQ Orbitrap mass spectrometer. FTIR spectra were acquired on a Bruker VECTOR22 infrared spectrophotometer. The absorption spectra of the dyes in solution and adsorbed on TiO_2 films (thickness 6 μm) at glass plates were recorded with a Shimadzu UV/Vis 2450 spectrophotometer. Absorption spectra dyes on TiO_2 were obtained through placing the dyes-adsorbing TiO_2 film at sample cell and the blank TiO_2 film at reference cell, in perpendicular to the light path.

The cyclic voltammograms were determined with a CHI620D electrochemical workstation (Shanghai Chenhua Instrument Company Limited) using a three-electrode cell with a glassy carbon working electrode, a Pt wire counter electrode, and a saturated calomel reference electrode (SCE). The supporting electrolyte was 0.1 M tetra-*n*-butylammonium hexafluorophosphate ($TBAPF_6$) in dichloromethane as the solvent.

The incident photo-to-current conversion efficiency (IPCE) of the DSSCs was measured using a 300 W Xe lamp light source with monochromatic light in the range of 300–800 nm. The photocurrent–voltage (*J*–*V*) characteristics of the solar cells were carried out using a Keithley 2420 3A source meter controlled by test-point software under solar simulator (solar AAA simulator, oriel USA, calibrated with a standard crystalline silicon solar). The total covered active electrode area with black mask of DSSCs was 0.25 cm^2.

2.2. Synthesis procedures and characterization data of new compounds

2.2.1. General procedure for the synthesis of ***1a–d***

A mixture of 9,10-phenanthrenedione derivative (10.0 mmol), either 4-bromobenzaldehyde or 2-thiophenecarboxaldehyde (10.3 mmol) and ammonium acetate (0.2 mol) in glacial acetic acid (100 mL) was heated to 100 °C for 1 h. After cooling, it was quenched with dilute ammonium hydroxide solution until pH 7. The precipitate was collected by filtration and washed with acetate acid, dilute sodium hydrogen carbonate solution and water, respectively. The white solid was further dried under reduced vacuum for 2 h.

*2.2.1.1. 2-(4-Bromophenyl)-1H-phenanthro[9,10-d]imidazole (**1a**).* White solid, yield: 98%. $R_f = 0.80$ (CH_2Cl_2). ^{1}H NMR (300 MHz, DMSO [D_6]): δ 13.52 (s, 1 H, NH), 8.89–8.83 (m, 2 H, ArH), 8.59–8.52 (m, 2 H, ArH), 8.26 (d, J = 7.5 Hz, 2 H, ArH), 7.82 (d, J = 7.6 Hz, 2 H, ArH), 7.76–7.64 (m, 4 H, ArH). ^{13}C NMR (75 MHz, DMSO [D_6]): δ 148.0, 137.0, 131.9, 129.6, 128.0, 127.7, 127.1, 125.3, 123.8, 122.5, 121.9. IR (KBr, cm^{-1}): 1621 (m), 1596 (m), 1472 (s), 1434 (m), 1227(s), 1171 (s), 1035 (s), 827 (m). TOFMS (EI) calcd for (M^+) $C_{21}H_{13}BrN_2$: 372.0262, found: 372.0252.

*2.2.1.2. 2-Thiophen-2-yl-1H-phenanthro[9,10-d]imidazole (**1b**).* White solid, yield: 91%. $R_f = 0.65$ (CH_2Cl_2). ^{1}H NMR (300 MHz, DMSO [D_6]): δ 13.55 (s, 1 H, NH), 8.86 (m, 2 H, ArH), 8.49 (m, 2 H, ArH), 7.94 (dd, J = 3.7 Hz, 1.1 Hz, 1 H, ArH), 7.93–7.62 (m, 5 H, ArH), 7.28 (dd, J = 5.0 Hz, 3.7 Hz, 1 H, ArH). ^{13}C NMR (75 MHz, DMSO [D_6]): δ 144.9, 133.9, 128.2, 127.7, 127.6, 127.1, 125.8, 125.2, 123.9, 121.9. IR (KBr, cm^{-1}): 1682 (s), 1486 (s), 1454 (s), 1410 (m), 1356 (m), 1277 (m), 754 (s), 703 (s). TOFMS (EI) calcd for (M^+) $C_{19}H_{12}N_2S$: 300.0721, found: 300.0685.

*2.2.1.3. 2-(4-Bromophenyl)-6,9-dimethoxy-1H-phenanthro[9,10-d] imidazole (**1c**).* White solid, yield: 96%. $R_f = 0.60$ (CH_2Cl_2). ^{1}H NMR (300 MHz, DMSO [D_6]): δ 13.35 (s, 1 H, NH), 8.45 (d, $J = 8.1$ Hz, 2 H, ArH), 8.23–8.20 (m, 4 H, ArH), 7.80 (d, $J = 8.4$ Hz, 2 H, ArH), 7.41 (m, 2 H, ArH), 4.02 (s, 6 H, OCH_3). ^{13}C NMR (75 MHz, DMSO [D_6]): δ 157.6, 147.4, 132.3, 130.2, 129.2, 128.2, 123.9, 122.5, 116.9, 107.1, 56.0. IR (KBr, cm^{-1}): 1623 (m), 1597 (m), 1470 (s), 1434 (m), 1406 (m), 1222 (s), 1172 (s), 1032 (s), 822 (m). TOFMS (EI) calcd for (M^+) $C_{23}H_{17}BrN_2O_2$: 432.0473, found: 432.0485.

*2.2.1.4. 6,9-Dimethoxy-2-thiophen-2-yl-1H-phenanthro[9,10-d]imidazole (**1d**).* White solid, yield: 90%. $R_f = 0.50$ (CH_2Cl_2). ^{1}H NMR (300 MHz, DMSO [D_6]): δ 13.33 (s, 1 H, NH), 8.38 (d, $J = 9.0$ Hz, 2 H, ArH), 8.22 (s, 2 H, ArH), 7.86 (dd, $J = 3.6$ Hz, 1.2 Hz, 1 H, ArH), 7.68 (dd, $J = 5.0$ Hz, 1.1 Hz, 1 H, ArH), 7.40 (m, 2 H, ArH), 7.26 (dd, $J = 5.0$ Hz, 3.7 Hz, 1 H, ArH), 4.03 (s, 6 H, OCH_3). ^{13}C NMR (75 MHz, DMSO [D_6]): δ 157.0, 143.9, 134.2, 128.7, 128.1, 127.2, 125.2, 123.3, 116.4, 106.6, 55.5. IR (KBr, cm^{-1}): 1624 (m), 1579 (m), 1466 (s), 1408 (m), 1232 (s), 1203 (s), 1174 (s), 1031 (m), 834 (m). TOFMS (EI) calcd for (M^+) $C_{21}H_{16}N_2O_2S$: 360.0932, found: 360.0887.

*2.2.2. General procedure for the synthesis of **2a–d***

1*H*-phenanthro[9,10-*d*]imidazole derivative (2.0 mmol) and NaOH (8.0 mmol) were added into DMSO (5 mL). The mixture was stirred at room temperature for 2 h. After addition of *n*-octyl bromide (3.0 mmol), the reaction was stirred at room temperature for another 25 min. The temperature was increased to 85 °C, and the reaction mixture was stirred at this temperature overnight. The mixture was diluted with water, extracted with CH_2Cl_2. The combined organic solution was dried ($MgSO_4$), and concentrated in *vacuo*. The residue was further purified by trituration with petroleum ether to give a solid.

*2.2.2.1. 2-(4-Bromophenyl)-1-octyl-1H-phenanthro[9,10-d]imidazole (**2a**).* White solid, yield: 90%. $R_f = 0.50$ (CH_2Cl_2/petroleum ether 2:1). ^{1}H NMR (300 MHz, $CDCl_3$): δ 8.85 (d, $J = 7.8$ Hz, 1 H, ArH), 8.77 (d, $J = 7.8$ Hz, 1 H, ArH), 8.71 (d, $J = 8.1$ Hz, 1 H, ArH), 8.26 (d, $J = 7.8$ Hz, 1 H, ArH), 7.73–7.61 (m, 8 H, ArH), 4.59 (t, $J = 7.5$ Hz, 2 H, CH_2), 1.94–1.87 (m, 2 H, CH_2), 1.24–1.78 (m, 10 H, CH_2), 0.85 (t, $J = 6.9$ Hz, 3 H, CH_3). ^{13}C NMR (75 MHz, $CDCl_3$): δ 151.4, 138.1, 132.0, 131.6, 130.1, 129.2, 128.2, 127.3, 126.8, 126.3, 125.6, 124.9, 124.4, 124.0, 123.4, 123.1, 122.6, 120.7, 46.9, 31.7, 30.2, 29.1, 28.9, 26.2, 22.7, 14.2. IR (KBr, cm^{-1}): 2925 (s), 1530 (m), 1466 (s), 1397 (m), 1359 (s), 1009 (m), 753 (s), 722 (s). TOFMS (EI) calcd for (M^+) $C_{29}H_{29}BrN_2$: 484.1514, found: 484.1511.

*2.2.2.2. 1-Octyl-2-thiophen-2-yl-1H-phenanthro[9,10-d]imidazole (**2b**).* White solid, yield: 82%. $R_f = 0.49$ (CH_2Cl_2/petroleum ether 2:1). ^{1}H NMR (300 MHz, $CDCl_3$): δ 8.84–8.79 (m, 2 H, ArH), 8.68 (d, $J = 8.1$ Hz, 1 H, ArH), 8.24 (d, $J = 8.1$ Hz, 1 H, ArH), 7.72–7.53 (m, 6 H, ArH), 7.24–7.21 (m, 1 H, ArH), 4.71 (t, $J = 7.8$ Hz, 2 H, CH_2), 2.11–2.01 (m, 2 H, CH_2), 1.43–1.26 (m, 10 H, CH_2), 0.87 (t, $J = 6.5$ Hz, 3 H, CH_3). ^{13}C NMR (75 MHz, $CDCl_3$): δ 145.8, 138.0, 132.5, 129.1, 128.1, 128.0, 127.6, 127.3, 127.2, 126.7, 126.5, 125.5, 124.7, 124.3, 123.1, 123.0, 122.8, 120.4, 46.8, 31.8, 30.3, 29.2, 28.9, 26.4, 22.7, 14.2. IR (KBr, cm^{-1}): 2921 (s), 1606 (m), 1521 (m), 1478 (s), 1448 (s), 1362 (s), 1359 (s), 851 (m), 756 (s), 689 (s). TOFMS (EI) calcd for (M^+) $C_{27}H_{28}N_2S$: 412.1973, found: 412.1957.

*2.2.2.3. 2-(4-Bromophenyl)-6,9-dimethoxy-1-octyl-1H-phenanthro[9,10-d]imidazole (**2c**).* White solid, yield: 93%. $R_f = 0.31$ (CH_2Cl_2/petroleum ether 2:1). ^{1}H NMR (300 MHz, $CDCl_3$): δ 8.74 (d, $J = 9.0$ Hz, 1 H, ArH), 8.15 (d, $J = 9.0$ Hz, 1 H, ArH), 8.01 (s, 1 H, ArH), 7.87 (s, 1 H, ArH), 7.68 (m, 4 H, ArH), 7.33 (d, $J = 9.0$ Hz, 1 H, ArH), 7.18 (m, 1 H, ArH), 4.67 (t, $J = 7.5$ Hz, 2 H, CH_2), 4.06 (s, 3 H, OCH_3), 3.99 (s, 3 H, OCH_3), 1.83 (m, 2 H, CH_2), 1.11 (m, 10 H, CH_2), 0.82 (t, $J = 6.9$ Hz, 3 H, CH_3). ^{13}C NMR (75 MHz, $CDCl_3$): δ 157.6, 156.6, 150.4, 136.7, 131.9, 131.5, 130.3, 130.1, 128.9, 125.2, 124.1, 123.7, 122.1, 118.0, 116.2, 115.6, 107.1, 105.9, 55.6, 55.5, 46.7, 31.7, 30.1, 29.1, 28.9, 26.2, 22.6, 14.1. IR (KBr, cm^{-1}): 2929 (s), 1620 (m), 1588 (m), 1465 (s), 1365 (m), 1230 (s), 1049 (m), 823 (m). TOFMS (EI) calcd for (M^+) $C_{31}H_{33}BrN_2O_2$: 544.1725, found: 544.1718.

*2.2.2.4. 6,9-Dimethoxy-1-octyl-2-thiophen-2-yl-1H-phenanthro[9,10-d]imidazole (**2d**).* white solid, yield: 84%. $R_f = 0.30$ (CH_2Cl_2/petroleum ether 2:1). ^{1}H NMR (300 MHz, $CDCl_3$): δ 8.68 (d, $J = 8.8$ Hz, 1 H, ArH), 8.10–8.08 (m, 2 H, ArH), 7.95 (s, 1 H, ArH), 7.51 (dd, $J = 5.1$ Hz, 0.9 Hz, 1 H, ArH), 7.48 (d, $J = 3.6$ Hz, 1 H, ArH), 7.33 (dd, $J = 8.8$ Hz, 2.4 Hz, 1 H, ArH), 7.28–7.25 (m, 1 H, ArH), 7.20 (dd, $J = 5.0$ Hz, 3.6 Hz, 1 H, ArH), 4.60 (t, $J = 7.8$ Hz, 2 H, CH_2), 4.01 (s, 3 H, OCH_3), 4.00 (s, 3 H, OCH_3), 2.01–1.95 (m, 2 H, CH_2), 1.45–1.35 (m, 10 H, CH_2), 0.87 (t, $J = 6.6$ Hz, 3 H, CH_3). ^{13}C NMR (75 MHz, $CDCl_3$): δ 157.6, 156.6, 144.8, 136.5, 132.4, 130.3, 128.9, 128.1, 127.8, 127.6, 125.5, 124.3, 121.9, 121.8, 117.8, 116.2, 115.5, 107.2, 105.8, 55.5, 55.4, 46.6, 31.7, 30.3, 29.1, 29.0, 26.4, 22.6, 14.1. IR (KBr, cm^{-1}): 2923 (s), 1617 (m), 1579 (m), 1479 (s), 1366 (m), 1235 (s), 841 (m). TOFMS (EI) calcd for (M^+) $C_{29}H_{32}N_2O_2S$: 472.2185, found: 472.2167.

*2.2.3. General procedure for the preparation of **3a–d***

1-*Alkyl*-1*H*-phenanthro[9,10-*d*]imidazole derivative (4.0 mmol) was dissolved in anhydrous THF (12 mL) under N_2 and cooled to −78 °C. *n*-BuLi (4.8 mmol) was added. The mixture was stirred at this temperature for 1 h, then $(CH_3O)_3B$ (12.0 mmol) was added and the mixture was left to stand for 16 h. HCl (20%, 10 mL) was added, and stirring was continued for 0.5 h. The solid was obtained by slow diffusion of water into the THF solution at room temperature. The precipitate was collected by filtration and washed with water (3 × 100 mL) and light petroleum (20 mL), respectively. The product was further dried under reduced vacuum for 2 h and the solid is pure enough for the next reaction.

*2.2.3.1. 4-(1-Octyl-1H-phenanthro[9,10-d]imidazol-2-yl)-phenylboronic acid (**3a**).* White solid, yield: 90%. $R_f = 0.70$ (CH_2Cl_2/CH_3OH 10:1). ^{1}H NMR (300 MHz, DMSO [D_6]): δ 9.07 (d, $J = 7.2$ Hz, 1 H, ArH), 8.97 (d, $J = 7.6$ Hz, 1 H, ArH), 8.67 (d, $J = 7.1$ Hz, 1 H, ArH), 8.49 (d, $J = 7.1$ Hz, 1 H, ArH), 8.10 (d, $J = 7.1$ Hz, 1 H, ArH), 7.90–7.77 (m, 7 H, ArH), 4.76 (t, $J = 7.2$ Hz, 2 H, CH_2), 1.87 (m, 2 H, CH_2), 1.09–1.04 (m, 10 H, CH_2), 0.78 (t, $J = 7.0$ Hz, 3 H, CH_3). IR (KBr, cm^{-1}): 1610 (s), 1469 (s), 1359 (s), 1278 (s), 753 (m), 723 (m). TOFMS (EI) calcd for (M^+) $C_{29}H_{31}BN_2O_2$: 450.2479, found: 450.2488.

*2.2.3.2. 5-(1-Octyl-1H-phenanthro[9,10-d]imidazol-2-yl)-thiophene-2-boronic acid (**3b**).* 97%. $R_f = 0.50$ (CH_2Cl_2/CH_3OH 10:1).^{1}H NMR (300 MHz, DMSO [D_6]): δ 9.02 (d, 1 H, $J = 7.6$ Hz, ArH), 8.91 (d, $J = 8.0$ Hz, 1 H, ArH), 8.66 (d, $J = 7.6$ Hz, 1 H, ArH), 8.45 (d, $J = 8.0$ Hz, 1 H, ArH), 7.87–7.70 (m, 6 H, ArH), 4.86(t, $J = 7.1$ Hz, 2 H, CH_2), 1.96 (m, 2 H, CH_2), 1.34–1.17 (m, 10 H, CH_2), 0.81 (t, $J = 6.7$ Hz, 3 H, CH_3). IR (KBr, cm^{-1}): 1613 (s), 1468 (s), 1359 (s), 1277 (s), 768 (m), 725 (m). TOFMS (EI) calcd for (M^+) $C_{27}H_{29}BN_2O_2S$: 456.2043, found: 456.1957.

*2.2.3.3. 4-(6,9-Dimethoxy-1-octyl-1H-phenanthro[9,10-d]imidazol-2-yl)-phenyl-boronic acid (**3c**).* White solid, yield: 86%. $R_f = 0.68$ (CH_2Cl_2/CH_3OH 10:1). ^{1}H NMR (300 MHz, DMSO [D_6]): δ 8.65 (d, $J = 8.7$ Hz, 1 H, ArH), 8.39–8.32 (m, 2 H, ArH), 8.27 (d, $J = 7.8$ Hz, 1 H, ArH), 8.10–7.90 (m, 4 H), 7.51–7.45 (m, 2 H, ArH), 4.63 (t, $J = 7.5$ Hz, 2 H, CH_2), 4.04 (s, 3 H, OCH_3), 4.02 (s, 3 H, OCH_3), 1.78 (m, 2 H, CH_2), 1.15–1.04 (m, 10 H, CH_2), 0.78 (t, $J = 7.0$ Hz, 3 H, CH_3). IR (KBr, cm^{-1}): 1610 (s), 1463 (s), 1362 (s), 1231 (s), 1044 (m), 1019 (m). TOFMS (EI) calcd for (M^+) $C_{31}H_{35}BN_2O_4$: 510.2690, found: 510.2598.

*2.2.3.4. 5-(6,9-Dimethoxy-1-octyl-1H-phenanthro[9,10-d]imidazol-2-yl)-thiophene-2-boronic acid (**3d**).* Green solid, yield: 93%. R_f = 0.46 (CH_2Cl_2/CH_3OH 10:1). ^1H NMR (300 MHz, DMSO [D_6]): δ 8.60 (d, J = 8.8 Hz, 1 H, ArH), 8.35–8.31 (m, 2 H, ArH), 8.24 (d, J = 2.1 Hz, 1 H, ArH), 7.88 (m, 2 H, ArH), 7.50–7.44 (m, 2 H, ArH), 4.78 (t, J = 7.1 Hz, 2 H, CH_2), 4.04 (s, 3 H, OCH_3), 4.03 (s, 3 H, OCH_3), 1.96–1.92 (m, 2 H, CH_2), 1.33–1.184 (m, 10 H, CH_2), 0.83 (t, J = 7.0 Hz, 3 H, CH_3). IR (KBr, cm^{-1}): 1613 (s), 1468 (s), 1359 (s), 1277 (s), 768 (m), 725 (m). TOFMS (EI) calcd for (M^+) $C_{29}H_{33}BN_2O_4S$: 516.2254, found: 516.2210.

*2.2.4. Preparation of **4**, **5** and **6***

*2.2.4.1. 5,5-Difluoro-1,3,7,9-tetramethyl-10-pentyl-5H-dipyrrolo[1,2-c:2′,1′-f] [1,3,2]diazaborinin-4-ium-5-uide (**4**) [51].* Oxalyl chloride (2.2 g, 17.3 mmol) in anhydrous CH_2Cl_2 (6 mL) was added dropwise to *n*-hexanoic acid (2.0 g, 17.2 mmol) in anhydrous CH_2Cl_2 (40 mL) over a period of 5 min. After stirring for 2 h the solution was concentrated to remove the unreacted oxalyl chloride and then obtain quantitative n-hexanoyl chloride. The resulting was dissolved in 50 mL anhydrous CH_2Cl_2 and 2, 4-dimethylpyrrole (3.3 g, 35 mmol) was added. The mixture was heated under reflux for 3 h. The solution was concentrated and the petroleum ether (100 mL) was added. A red precipitate had appeared and was dissolved in 60 mL toluene. Triethylamine (5 mL) was then added and the solution turned brown-yellow. After 10 min, boron trifluoride etherate (5 mL) was added and the reaction mixture stirred for 1 h at room temperature. Then, the mixture was washed with 50 mL of saturated aqueous NaCl there times, dried over $MgSO_4$ and concentrated. The product was purified by column chromatography to give a red-brown solid (1.4 g, 25%). R_f = 0.53 (CH_2Cl_2/petroleum ether 1:2). ^1H NMR (300 MHz, $CDCl_3$): δ 6.05 (s, 2 H, ArH), 2.96–2.91 (m, 2 H, CH_2), 2.51 (s, 6 H, CH_3), 2.41 (s, 6 H, CH_3), 1.69–1.58 (m, 2 H, CH_2), 1.52–1.33 (m, 4 H, CH_2), 0.96–0.91 (t, J = 7.2 Hz, 3 H, CH_3). ^{13}C NMR ($CDCl_3$, 75 MHz): δ 153.5, 146.6, 140.2, 131.3, 121.4, 32.4, 31.4, 28.2, 22.3, 16.1, 14.2, 13.9. IR (KBr, cm^{-1}): 2960 (m), 2927 (m), 1548 (s), 1507 (s), 1196 (s), 1074 (s), 982 (s), 808 (s). TOFMS (EI) calcd for (M^+) $C_{18}H_{25}BF_2N_2$: 318.2079, found 318.2076.

*2.2.4.2. 5,5-Difluoro-8-formyl-1,3,7,9-tetramethyl-10-pentyl-5H-dipyrrolo[1,2-c:2′,1′-f] [1,3,2]diazaborinin-4-ium-5-uide (**5**) [52].* $POCl_3$ (6 mL) was added dropwise to DMF (10 mL) in an ice bath for 5 min under N_2. The solution was stirred for additional 30 min at room temperature. Compound **4** (0.64 g, 2.0 mmol) in $ClCH_2CH_2Cl$ (30 mL) was added and the temperature was increased to 50 °C. The mixture was stirred for an additional 45 min. The reaction mixture was cooled to room temperature and slowly poured into K_2CO_3 solution (100 mL) under ice-cold conditions. After being warmed to room temperature, the reaction mixture was further stirred for 30 min and washed with water. The organic layers were combined, dried over anhydrous $MgSO_4$, and evaporated in vacuo. The crude product was further purified using column chromatography to give **8** as a yellow solid. Yield: 90%. R_f = 0.28 (CH_2Cl_2/petroleum ether 1:1). ^1H NMR (300 MHz, $CDCl_3$): δ 10.11 (s, 1 H, CHO), 6.23 (s, 1 H, ArH), 3.05 (t, J = 7.7 Hz, 2 H, CH_2), 2.78 (s, 3 H, CH_3), 2.75 (s, 3 H, CH_3), 2.58 (s, 3 H, CH_3), 2.48 (s, 3 H, CH_3), 1.67 (m, 2 H, CH_2), 1.53–1.36 (m, 4 H, CH_2), 0.94 (t, J = 7.2 Hz, 3 H, CH_3). ^{13}C NMR (75 MHz, $CDCl_3$): δ 186.0, 159.7, 155.3, 148.9, 144.7, 139.5, 134.2, 129.9, 125.9, 124.5, 32.4, 31.4, 28.5, 22.5, 16.8, 14.8, 14.0, 12.7, 12.6. IR (KBr, cm^{-1}): 2921 (m), 1664 (s), 1527 (s), 1197 (s), 995 (s), 765 (m). TOFMS (EI) calcd for (M^+) $C_{19}H_{25}BF_2N_2O$: 346.2028, found: 346.2026.

*2.2.4.3. 5,5-Difluoro-8-formyl-2-iodo-1,3,7,9-tetramethyl-10-pentyl-5H-dipyrrolo[1,2-c:2′,1′-f] [1,3,2]diazaborinin-4-ium-5-uide(**6**) [53].* ICl (0.24 g, 1.5 mmol) in MeOH (5 mL) was added dropwise to **5** (0.41 g, 1.2 mmol) in a DMF/MeOH (10 mL/10 mL) mixture over a period of 5 min. After stirring for 1 h, water was added (20 mL). The mixture was extracted with CH_2Cl_2. The organic layer was washed with $Na_2S_2O_3$ solution (10%), dried by $MgSO_4$, and evaporated in vacuo. The residue was purified by column chromatography to give product as a red solid. Yield: 93%. R_f = 0.42 (CH_2Cl_2/petroleum ether 1:1). ^1H NMR (300 MHz, $CDCl_3$): δ 10.13 (s, 1H, CHO), 3.09 (t, J = 8.4 Hz, 2 H, CH_2), 2.79 (s, 3 H, CH_3), 2.76 (s, 3 H, CH_3), 2.67 (s, 3 H, CH_3), 2.53 (s, 3 H, CH_3), 1.65 (m, 2 H, CH_2), 1.52–1.37 (m, 4 H, CH_2), 0.95 (t, J = 7.1 Hz, 3 H, CH_3). ^{13}C NMR (75 MHz, $CDCl_3$): δ 185.9, 158.8, 156.6, 149.3, 144.9, 142.0, 133.6, 130.1, 126.3, 89.0, 32.3, 31.3, 29.0, 22.4, 19.3, 16.4, 14.0, 13.1, 12.9. IR (KBr, cm^{-1}): 2925 (m), 1665 (s), 1528 (s), 1348 (s), 1198 (s), 997 (s), 761 (m). TOFMS (EI) calcd for (M^+) $C_{19}H_{24}BF_2N_2OI$: 472.0995, found 472.0984.

*2.2.5. General procedure for the preparation of **7a–d***

The above boronic acid (0.6 mmol), BODIPY **6** (0.5 mmol), K_2CO_3 solution (2 M, 3 mL), THF (15 mL), toluene (15 mL) and $Pd(PPh_3)_4$ (50 mg) were added into a flask (50 mL). The mixture was heated under reflux overnight under N_2. After evaporating the solvent under reduced pressure, H_2O (50 mL) and CH_2Cl_2 (100 mL) were added. The organic layer was separated and dried in $MgSO_4$. The solvent was removed under reduced pressure. The according aldehyde derivative was obtained by column chromatography on silica gel using CH_2Cl_2 and EtOAc.

*2.2.5.1. Compound **7a**.* Red solid, yield: 85%. R_f = 0.35 (CH_2Cl_2/EtOAc 200:1). ^1H NMR (300 MHz, $CDCl_3$): δ 10.15 (s, 1 H, CHO), 8.86 (d, J = 7.2 Hz, 1 H, ArH), 8.72 (d, J = 8.0 Hz, 1 H, ArH), 8.29 (d, J = 8.4 Hz, 1 H, ArH), 7.88 (d, J = 8.0 Hz, 2 H, ArH), 7.73–7.65 (m, 5 H, ArH), 7.42 (d, J = 7.6 Hz, 2 H, ArH), 4.70 (t, J = 7.2 Hz, 2 H, CH_2), 3.16 (m, 2 H, CH_2), 2.83–2.80 (m, 6 H, CH_3), 2.59 (s, 3 H, CH_3), 2.45 (s, 3 H, CH_3), 1.98 (m, 2 H, CH_2), 1.56–1.50 (m, 4 H, CH_2), 1.47–1.38 (m, 2 H, CH_2), 1.27–1.17 (m, 10 H, CH_2), 0.96 (t, J = 7.2 Hz, 3 H, CH_3), 0.83 (t, J = 7.0 Hz, 3 H, CH_3). ^{13}C NMR (75 MH_Z, $CDCl_3$): δ 186.2, 158.1, 156.0, 152.1, 149.6, 140.2, 135.7, 134.0, 130.7, 130.3, 129.2, 128.2, 127.3, 126.8, 126.3, 126.2, 125.6, 124.9, 124.5, 123.4, 123.1, 122.6, 120.8, 47.0, 32.5, 31.7, 31.6, 30.3, 29.0, 28.8, 26.3, 22.6, 22.5, 14.9, 14.1, 13.8, 13.0, 12.8. IR (KBr, cm^{-1}): 1667 (s), 1530 (s), 1387 (m), 1321 (s), 1228 (s), 1075 (s) 1020 (m), 998 (m). TOFMS (ESI) calcd for ($[M + H]^+$) $C_{48}H_{54}BF_2N_4O$: 751.4353, found: 751.4349.

*2.2.5.2. Compound **7b**.* Dark solid, yield: 80%. R_f = 0.45 (CH_2Cl_2/EtOAc 200:1). ^1H NMR (300 MHz, $CDCl_3$): δ 10.14 (s, 1 H, CHO), 8.85 (d, J = 7.0 Hz, 2 H, ArH), 8.69 (d, J = 8.1 Hz, 1 H, ArH), 8.27 (d, J = 7.5 Hz, 1 H, ArH), 7.68–7.66 (m, 5 H, ArH), 7.07 (m, 1 H, ArH), 4.80 (t, J = 7.2 Hz, 2 H, CH_2), 3.13 (m, 2 H, CH_2), 2.82–2.78 (m, 6 H, CH_3), 2.67 (s, 3 H, CH_3), 2.55 (s, 3 H, CH_3), 2.14 (m, 2 H, CH_2), 1.51–1.28 (m, 16 H, CH_2), 0.96 (t, J = 6.8 Hz, 3 H, CH_3), 0.87 (t, J = 6.7 Hz, 3 H, CH_3). ^{13}C NMR (75 MHz, $CDCl_3$): δ 186.0, 158.0, 156.5, 150.1, 145.3, 141.3, 141.1, 138.1, 136.1, 133.8, 133.5, 130.5, 129.3, 129.2, 128.3, 128.2, 127.9, 127.3, 127.1, 126.9, 126.8, 126.4, 125.7, 125.1, 124.5, 123.1, 123.0, 122.8, 120.5, 47.1, 32.4, 31.7, 31.5, 30.5, 29.2, 29.0, 28.8, 26.5, 22.6, 22.4, 15.0, 14.1, 14.0, 13.9, 13.0, 12.8. IR (KBr, cm^{-1}): 1671 (s), 1538 (s), 1455 (m), 1362 (m), 1322 (m), 1205 (s), 1018 (m). TOFMS (ESI) calcd for ($[M + H]^+$) $C_{46}H_{52}BF_2N_4OS$: 757.3918, found: 757.3916.

*2.2.5.3. Compound **7c**.* Red solid, yield: 86%. R_f = 0.23 (CH_2Cl_2/EtOAc 200:1). ^1H NMR (300 MHz, $CDCl_3$): δ 10.15 (s, 1 H, CHO), 8.76 (m, 1 H, ArH), 8.21–8.15 (m, 2 H, ArH), 8.01 (s, 1 H, ArH), 7.87 (d, J = 7.2 Hz, 2 H, ArH), 7.42–7.34 (m, 4 H, ArH), 4.66 (m, 2 H, CH_2), 4.06 (s, 3 H, OCH_3), 4.01 (s, 3 H, OCH_3), 3.14 (m, 2 H, CH_2), 2.82–2.78 (m, 6 H, CH_3), 2.59 (s, 3 H, CH_3), 2.45 (s, 3 H, CH_3), 1.96 (m, 2 H, CH_2), 1.51–1.41 (m, 6 H, CH_2), 1.18 (m, 10 H, CH_2), 0.96 (t, J = 6.9 Hz, 3 H, CH_3), 0.83 (t, J = 6.5 Hz, 3 H, CH_3). ^{13}C NMR (75 MHz, $CDCl_3$): δ 186.1, 158.1, 157.7, 156.7, 155.9, 151.2, 149.5, 140.1, 136.8, 135.6, 134.6, 133.8,

130.7, 130.6, 130.4, 130.2, 129.0, 126.1, 125.3, 124.1, 122.2, 118.2, 116.4, 115.7, 107.3, 106.0, 55.6, 55.5, 46.8, 32.5, 31.7, 31.5, 30.2, 29.7, 29.0, 28.8, 26.3, 22.6, 22.5, 14.8, 14.0, 13.8, 13.0, 12.7. IR (KBr, cm^{-1}): 1666 (s), 1538 (s), 1469 (s), 1322 (m), 1230 (m), 1198 (m), 1075 (m), 1025 (m). TOFMS (ESI) calcd for ($[M + H]^+$) $C_{50}H_{58}BF_2N_4O_3$: 811.4565, found: 811.4561.

2.2.5.4. Compound ***7d***. Dark solid, yield: 83%. R_f = 0.36 (CH_2Cl_2/EtOAc 200:1). ^1H NMR (300 MHz, $CDCl_3$): δ 10.14 (s, 1 H, CHO), 8.77 (m, 1 H, ArH), 8.18–8.14 (m, 2 H, ArH), 7.99 (s, 1 H, ArH), 7.39–7.32 (m, 3 H, ArH), 7.06 (m, 1 H, ArH), 4.75 (m, 2 H, CH_2), 4.05 (s, 3 H, OCH_3), 4.03 (s, 3 H, OCH_3), 3.12 (m, 2 H, CH_2), 2.82–2.78 (m, 6 H, CH_3), 2.66 (s, 3 H, CH_3), 2.54 (s, 3 H, CH_3), 2.10 (m, 2 H, CH_2), 1.53–1.26 (m, 16 H, CH_2), 0.95 (t, J = 7.1 Hz, 3 H, CH_3), 0.87 (t, J = 6.3 Hz, 3 H, CH_3). ^{13}C NMR (75 MHz, $CDCl_3$): δ. 186.1, 158.0, 157.8, 156.8, 156.4, 150.0, 144.3, 141.3, 136.8, 135.8, 134.5, 1347.1, 133.5, 130.5, 129.2, 129.0, 128.4, 128.0, 126.3, 125.8, 124.3, 122.0, 117.8, 116.3, 115.6, 107.4, 105.9, 55.6, 55.9, 46.9, 32.4, 31.7, 31.4, 30.4, 29.7, 29.2, 29.1, 28.8, 26.5, 22.6, 22.4, 15.0, 14.0, 13.9, 13.0, 12.8. IR (KBr, cm^{-1}): 1670 (s), 1537 (s), 1465 (s), 1323 (m), 1231 (m), 1177 (m), 1064 (m), 1020 (m). TOFMS (ESI) calcd for ($[M + H]^+$) $C_{48}H_{56}BF_2N_4O_3S$: 817.4129, found: 817.4124.

2.2.6. General procedure for the preparation of ***PB1–4*** *and compound* ***8***

The aldehyde derivative (0.15 mmol), dissolved in $CHCl_3$ (15 mL) and CH_3CN (15 mL), was condensed with 2-cyanoacetic acid (0.30 mmol) in the presence of piperidine (1.2 μmol). The mixture was heated under reflux for 24 h under a nitrogen atmosphere. After cooling to room temperature, the mixture was poured to CH_2Cl_2 (50 mL) and washed with water (2 × 50 mL). Organic phase was dried over $MgSO_4$ and solvent was evaporated and the residue was purified by silica gel column chromatography using CH_2Cl_2 and MeOH as the eluant.

2.2.6.1. Dye ***PB1***. Dark red solid, yield: 80%. R_f = 0.55 (CH_2Cl_2/CH_3OH 1:2). ^1H NMR (300 MHz, $CDCl_3$): δ 8.86 (m, 1 H, ArH), 8.74–8.71 (m, 1 H, ArH), 8.31 (d, J = 7.8 Hz, 1 H, ArH), 8.13 (s, 1 H, CH), 7.93 (m, 2 H, ArH), 7.74 (m, 5 H, ArH), 7.48 (m, 2 H, ArH), 4.75 (m, 2 H, CH_2), 3.10 (m, 2 H, CH_2), 2.55 (s, 6 H, CH_3), 2.45 (s, 6 H, CH_3), 2.04 (m, 2 H, CH_2), 1.70 (m, 2 H, CH_2), 1.52–1.43 (m, 4 H, CH_2), 1.25–1.20 (m, 10 H, CH_2), 0.96 (t, J = 6.9 Hz, 3 H, CH_3), 0.83 (t, J = 6.6 Hz, 3 H, CH_3). IR (KBr, cm^{-1}): 1714 (m), 1539 (s), 1466 (m), 1396 (m), 1196 (m), 1075 (m), 1016 (s). TOFMS (ESI) calcd for ($[M + H]^+$) $C_{51}H_{55}BF_2N_5O_2$: 818.4411, found: 818.4412.

2.2.6.2. Dye ***PB2***. Dark solid, yield: 79%. R_f = 0.58 (CH_2Cl_2/CH_3OH 1:2). ^1H NMR (300 MHz, $CDCl_3$): δ 8.88–8.85 (m, 2 H, ArH), 8.71 (d, J = 8.4 Hz, 1 H, ArH), 8.29 (d, J = 7.8 Hz, 1 H, ArH), 8.26 (s, 1 H, CH), 7.77–7.61 (m, 5 H, ArH), 7.09 (d, J = 3.4 Hz, 1 H, ArH), 4.81 (m, 2 H, CH_2), 3.09 (m, 2 H, CH_2), 2.65 (s, 3 H, CH_3), 2.62 (s, 3 H, CH_3), 2.53 (s, 3 H, CH_3), 2.49 (s, 3 H, CH_3), 2.14 (m, 2 H, CH_2), 1.69 (m, 2 H, CH_2), 1.52–1.28 (m, 14 H, CH_2), 0.95 (t, J = 7.0 Hz, 3 H, CH_3), 0.88 (t, J = 6.7 Hz, 3 H, CH_3). IR (KBr, cm^{-1}): 1714 (m), 1537 (s), 1470 (m), 1362 (m), 1203 (s), 1072 (m), 1013 (s). TOFMS (ESI) calcd for ($[M + H]^+$) $C_{49}H_{53}BF_2N_5O_2S$: 824.3976, found: 824.3970.

2.2.6.3. Dye ***PB3***. Dark red solid, yield: 82%. R_f = 0.54 (CH_2Cl_2/CH_3OH 1:2). ^1H NMR (300 MHz, $CDCl_3$): δ 8.74 (s, 1 H, ArH), 8.27–8.16 (m, 3 H, ArH), 8.14 (s, 1 H, CH), 8.02 (s, 1 H, ArH), 7.87 (d, J = 7.2 Hz, 1 H, ArH), 7.41–7.37 (m, 4 H, ArH), 4.76 (m, 2 H, CH_2), 4.08 (s, 3 H, OCH_3), 4.06 (s, 3 H, OCH_3), 3.12 (m, 2 H, CH_2), 2.57 (s, 6 H, CH_3), 2.47 (s, 6 H, CH_3), 2.08 (m, 2 H, CH_2), 1.70–1.43 (m, 6 H, CH_2), 1.25–1.20 (m, 10 H, CH_2), 0.95 (t, J = 6.9 Hz, 3 H, CH_3), 0.83 (t, J = 6.6 Hz, 3 H, CH_3). IR (KBr, cm^{-1}): 1728 (m), 1538 (s), 1466 (m), 1231 (s), 1196 (s), 1076 (m), 1018 (s). TOFMS (ESI) calcd for ($[M + H]^+$) $C_{53}H_{59}BF_2N_5O_4$: 878.4623, found: 878.4620.

2.2.6.4. Dye ***PB4***. Dark solid, yield: 77%. R_f = 0.55 (CH_2Cl_2/CH_3OH 1:2). ^1H NMR (300 MHz, $CDCl_3$): δ 8.72 (m, 1 H, ArH), 8.26 (s, 1 H, CH), 8.21–8.17 (m, 2 H, ArH), 8.01 (s, 1 H, ArH), 7.55 (m, 1 H, ArH), 7.41–7.34 (m, 2 H, ArH), 7.08 (m, 1 H, ArH), 4.77 (m, 2 H, CH_2), 4.06 (s, 3 H, OCH_3), 4.04 (s, 3 H, OCH_3), 3.08 (m, 2 H, CH_2), 2.64 (s, 3 H, CH_3), 2.63 (s, 3 H, CH_3), 2.52 (s, 3 H, CH_3), 2.49 (s, 3 H, CH_3), 2.11 (m, 2 H, CH_2), 1.58–1.26 (m, 16 H, CH_2), 0.95 (t, J = 7.0 Hz, 3 H, CH_3), 0.88 (t, J = 6.8 Hz, 3H, CH_3). IR (KBr, cm^{-1}): 1714 (m), 1620 (m), 1538 (s), 1467 (m), 1202 (s), 1177 (s), 1073 (m), 1014 (s). TOFMS (ESI) calcd for ($[M + H]^+$) $C_{51}H_{57}BF_2N_5O_4S$: 884.4187, found: 884.4193.

*2.2.6.5. (E)-8-(2-carboxy-2-cyanovinyl)-5,5-difluoro-1,3,7,9-tetramethyl-10-pentyl-5H-dipyrrolo[1,2-c:2′,1′-f] [1,3,2]diazaborinin-4-ium-5-uide (****8****).* Red solid, yield: 88%. R_f = 0.30 (CH_2Cl_2/CH_3OH 10:1). ^1H NMR (300 MHz, DMSO[D_6]): δ 8.27 (s, 1 H, CH), 6.46 (s, 1 H, ArH), 3.06 (t, J = 7.7 Hz, 2 H, CH_2), 2.54–2.44 (m, 12 H, CH_3), 1.60 (m, 2 H, CH_2), 1.53–1.36 (m, 4 H, CH_2), 0.88 (t, J = 7.2 Hz, 3 H, CH_3). ^{13}C NMR (75 MHz, DMSO[D_6]): δ 163.0, 158.5, 150.3, 148.5, 148.1, 144.8, 137.1, 132.9, 130.2, 124.2, 123.6, 116.1, 107.1, 31.7, 30.9, 27.9, 21.7, 16.2, 14.9, 14.4, 13.8. IR (KBr, cm^{-1}): 2925 (m), 1665 (s), 1528 (s), 1348 (s), 1198 (s), 997 (s), 761 (m). TOFMS (ESI) calcd for ($[M + H]^+$) $C_{22}H_{27}BF_2N_3O_2$: 414.2164, found 414.2134.

2.3. Fabrication of dye-sensitized solar cells

DSSC was assembled in a sandwich configuration. The preparation of nanostructured TiO_2 films followed by hydrolysis of titanium tetraisopropoxide as described elsewhere [54]. Nanocrystalline electrodes, about 14.5 μm thickness [determined by a profilometer (XP-2, AMBIOS Technology Inc.)], were obtained by screen-printing TiO_2 paste on a Fluorine-doped SnO_2 (FTO) glass (TEC-8, LOF) and then sintering at 450 °C for 30 min in air. After cooling to 80 °C, the photoelectrode was immersed in a $CHCl_3$ solution (0.3 mM) of the dye **PB1–4** overnight at room temperature for 12 h. The excess of dye in TiO_2 films was rinsed off with anhydrous ethanol. The platinized counter electrodes were obtained by spraying H_2PtCl_6 solution to FTO glass followed by heating at 410 °C for 20 min. Then, the counter electrode was placed directly on the top of the dye-sensitized TiO_2 film. The gap between the electrodes was sealed by thermal adhesive films (Surlyn, Dupont). And the electrolyte was filled from a hole made on the counter electrode, which was later sealed by a cover glass and thermal adhesive films. DSSCs were fabricated with an effective area of 0.25 cm^2 and electrolyte composed of 0.6 M 1,2-dimethyl-3-*n*-propylimidazolium iodide (DMPImI), 0.1 M LiI, 0.05 M I_2 and 0.5 M *tert*-butyl pyridine (TBP) in acetonitrile.

3. Result and discussion

3.1. Synthesis of dyes ***PB1–4***

The synthetic strategy employed to access the target compounds **PB1–4** is shown in Scheme 1. First, compounds **1a–d** can be obtained by condensation of phenanthrenequinone derivatives with the corresponding aldehydes in the presence of ammonium acetate in acetic acid according to literature method [55], and then react with 1-bromooctane to form 1-*n*-octyl-1*H*-phenanthro [9,10-*d*]imidazole (**2**), which can be converted into the corresponding boronic acids **3** by reacting with *n*-BuLi, and subsequent addition of trimethyl borate at low temperature and a final acid

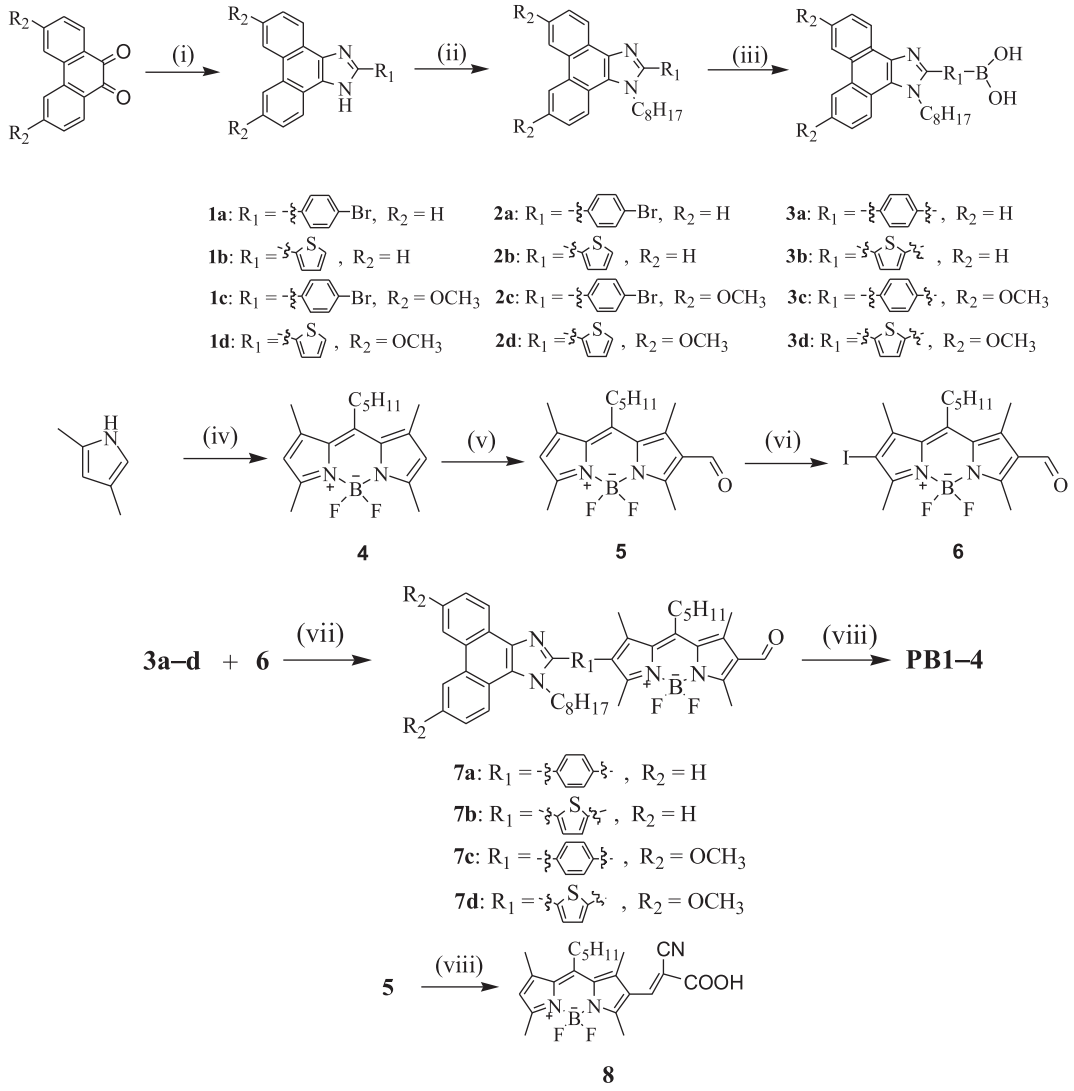

Scheme 1. Synthetic route to the BODIPY dyes.

hydrolysis at room temperature. Second, synthesis of BODIPY moiety starts from 2,4-dimethylpyrrole, and undergoes three steps to the 2-iodo-6-formyl BODIPY (**6**), shown in Scheme 1. Third, the coupling between the donor boronic acid (**3**) and the iodo conjugated bridge (**6**) was performed in the presence of $Pd(PPh_3)_4$ catalyst to produce the corresponding aldehydes **7** in excellent yields. Finally, the target dyes **PB1**–**4** were obtained from condensation of **7** with cyanoacetic acid in the presence of a catalytic amount of piperidine.

3.2. Photophysical properties

In general, the BODIPY dyes show absorption maxima in two widely separated regions (Fig. 2). The absorption spectra of the dyes **PB1**–**4** in $CHCl_3$ exhibit intense absorption in two regions bands 250–420 nm and 420–620 nm with an almost identical long wavelength absorption maximum at 532 nm, which is a typical BODIPY band. The absorption spectra of the thiophene containing dyes **PB2** and **PB4** are broader and more intense than those of the phenylene containing dyes **PB1** and **PB3**, relative data are listed in Table 1. The difference between the phenyl and thiophene substituted BODIPYs derives from a higher coplanarity of the thiophene unit with the BODIPY core. In other words, there is better conjugation between BODIPY unit and thiophene moiety over phenylene moiety due to smaller steric hindrance between 5,7-methyl groups of BODIPY unit and thiophene than phenylene. Compared with the unmodified BODIPY **4**, the absorption maxima

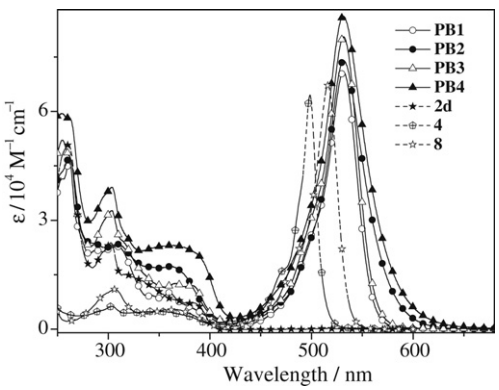

Fig. 2. Absorption spectra of the dyes **PB1**–**4**, **2d**, **4** and **8** in $CHCl_3$.

Table 1
Photophysical and electrochemical data of BODIPY dyes.

Dye	λ_{max} (solution) (nm)[a]	ε_{max} (M^{-1} cm^{-1})	λ_{max} (TiO_2) (nm)[b]	E_{ox}(V)[c] *vs* NHE	$E_{0,0}$(eV)[d] (λ_{onset} [nm])	E^*_{ox}(V)[e] *vs* NHE	E_{HOMO}[f] (eV)	E_{LUMO} (eV)
PB1	532(522)	71,100	523	1.38	2.09(594)	−0.71	−5.88	−3.79
PB2	532(522)	74,200	523	1.29	1.97(630)	−0.68	−5.79	−3.82
PB3	532(522)	86,900	523	1.17	2.05(604)	−0.88	−5.67	−3.62
PB4	532(522)	80,400	~523	1.11	1.92(645)	−0.81	−5.61	−3.69

[a] Absorption maximum in $CHCl_3$ (CH_3CN) solutions.
[b] Absorption maximum on TiO_2 were obtained through measuring the dyes adsorbed on 6 μm TiO_2 nanoparticle films in a $CHCl_3$ solution.
[c] E_{ox} determined by CV, in 0.10 M Bu_4NPF_6–CH_2Cl_2, and ferrocene as an external reference.
[d] $E_{0,0}$ was estimated from the absorption thresholds from absorption spectra of dyes absorbed on the TiO_2 film, $E_{0,0} = 1242.37/\lambda_{onset}$.
[e] Computed from the formula $E^*_{ox} = E_{ox} - E_{0,0}$.
[f] $E_{HOMO} = -4.5 - E_{ox}$.

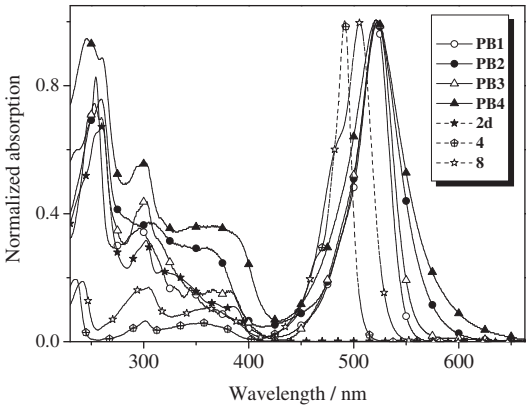

Fig. 4. Normalized absorption spectra of the dyes **PB1**–**4**, **2d**, **4** and **8** in CH_3CN.

of these dyes is red-shifted by about 33 nm. To check influence of cyanoacrylate group in the 2-poistion on the BODIPY absorption, the 2-cyanoacrylate BODIPY (**8**) has been prepared with **5** as the starting material. Relative to the BODIPY **8**, the absorption maxima of these dyes **PB1**–**4** have a red-shift of 16 nm. Hence, the 2,6-modification involving cyanoacrylic acid and either a 2,5-thienyl or 1,4-phenylene extended the conjugation pathway of the BODIPY core.

Normalized absorption spectra of dyes **PB1**–**4** adsorbed on TiO_2 film were obtained from the same TiO_2 film (6 μm) for solar cells, shown in Fig. 3. Compared with liquid spectra in $CHCl_3$, the solid-state absorption maxima have a small blue-shift (about 9 nm), smaller shoulders at higher energy appear, and the long wavelength absorption bands become broad. The latter is attributed to H-type aggregation on the TiO_2 surface and/or the dye-TiO_2 interaction [7,48,56]. To understand the origin of the blue-shift, UV/Vis absorption spectra of the foregoing compounds in a polar solvent, acetonitrile, were determined (Fig. 4). Except for **2d**, the UV/Vis absorption spectra in acetonitrile exhibit blue-shifts of ca. 11 nm for **PB1**–**4**, 10 nm for **8** and 7 nm for **4**, relative to those in the low-polar solvent. Thus, this shows that the electron contribution of these BODIPY derivatives in the excited states is more delocalized than in the ground states, namely dipole moments in the excited states become smaller.

3.3. Electrochemical properties

To evaluate the feasibility of electron injection from the excited-state molecule to the conduction band of TiO_2, the electrochemical behavior of dyes **PB1**–**4** has been examined by cyclic voltammetry (CV) using a standard three-electrode cell in an electrolyte solution 0.1 M tetrabutylammonium hexafluorophosphate ($TBAPF_6$) dissolved in dichloromethane. The working electrode is glassy carbon, the counter electrode is a platinum wire, and the reference electrode is the saturated calomel electrode (SCE). The CV voltammograms are shown in Fig. 5, using ferrocene as a standard. The half-wave oxidation potentials (E_{ox}) were obtained, and the excited-state oxidation potentials (E^*_{ox}) were estimated by subtracting the 0,0 transition energy ($E_{0,0}$) from E_{ox}, and data were listed in Table 1. The oxidation potentials (E_{ox}) of these compounds, ranging from 1.11 to 1.38 V *vs* NHE, are more positive than the iodide/tri-iodide redox couple (about 0.42 V *vs* NHE), indicating that the oxidized dye formed after election injection into the conduction band of TiO_2 can be regenerated from the reduced species in the electrolyte. The excited-state oxidation potential (E^*_{ox}), ranging from −0.68 to −0.88 V *vs* NHE, are higher than the conduction band of TiO_2 (about −0.5 V *vs* NHE), thus ensuring facile electron injection from the excited-state molecule to the TiO_2 conduction band. As a result, electron cycle of cells based on dyes **PB1**–**4** is fully available. Among them, the donor with electron-donating group(methoxy), for **PB3** and **PB4**, give lower oxidation potentials than those for **PB1** and **PB2**. Namely, introduction of the methoxy can elevate on the HOMO and LUMO levels of dyes, **PB3** and **PB4**. In addition, the electron-rich thiophene moiety contributes a lower E_{ox} than the phenylene, **PB2** *vs* **PB1** and **PB4** *vs* **PB3** (Table 1).

3.4. Photovoltaic performance of DSSCs based on the BODIPY dyes

Dye-sensitized solar cells were prepared with these dyes as sensitizers. Typical solar cells, with an effective area of 0.25 cm^2, are

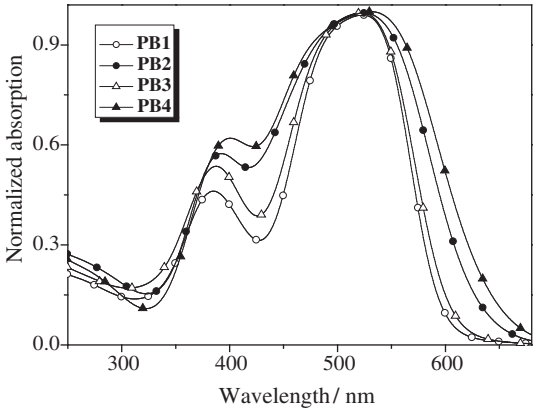

Fig. 3. Normalized absorption spectra of the dye **PB1**–**4** adsorbed on TiO_2 films.

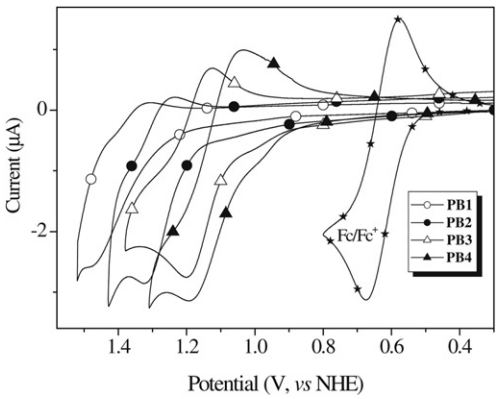

Fig. 5. Cyclic voltammogram of the dyes **PB1**–**4** in CH_2Cl_2 solutions.

Table 2
Photovoltaic performance of DSSCs based on the BODIPY series of dyes.[a]

Dye	J_{sc} (mA/cm^2)	V_{oc} (V)	*FF*	η (%)
PB1	1.12	0.51	0.57	0.33
PB2	1.20	0.50	0.54	0.33
PB3	2.64	0.54	0.64	0.92
PB4	3.20	0.58	0.69	1.30
PB4[b]	5.10	0.61	0.72	2.26

[a] Light source: 100 mW/cm^2, AM 1.5G simulated solar light; working area: 0.25 cm^2; thickness: 14.5 μm; dye bath: $CHCl_3$ solution (0.3 mM); electrolyte: 0.05 M I_2 + 0.1 M LiI + 0.6 M DMPImI + 0.5 M TBP in CH_3CN solution, unless other indicated.
[b] From an optimized fabrication process but not for the dye.

fabricated with 0.6 M DMPImI/0.05 M I_2/0.1 M LiI/0.5 M TBP in acetonitrile solution as an electrolyte. The detailed parameters of photovoltaic performance, short-circuit current density (J_{sc}), open-circuit voltage (V_{oc}), fill factor (*FF*), and photovoltaic conversion efficiency (η), are summarized in Table 2 and the corresponding photocurrent–voltage (*J*–*V*) curves are depicted in Fig. 6. Among the four dyes, the **PB4**-sensitized cell exhibited the best photovoltaic performance.

Based on these parameters, the electron-donating ability of the donor in a dye molecule plays a key role. The electron-donating ability of donor groups is indicated by the oxidation potentials. E_{ox} values of **PB3** and **PB4** which are lower than those of **PB1** and **PB2**. Higher HOMO and LUMO energy levels of **PB3** and **PB4** relative to **PB1** and **PB2** could not only generate effectively charge separation, but also accelerate the dye regeneration via fast oxidation of tri-iodide by oxidized dyes, to avoid charge recombination between oxidized dyes and photo-injected electrons in the nanocrystalline TiO_2 film, thus enhancing the sensitized cell performance. In addition, the electron-rich thiophene bridge also has an electron-donating ability based on E_{ox} values of **PB2** and **PB4** which are lower than those of **PB1** and **PB3**, respectively.

Absorption spectra of these dyes both in solutions and adsorbed on a TiO_2 film exhibit higher molar extinction coefficients and broader absorption bands for **PB2** and **PB4** over **PB1** and **PB3**. However, the **PB2**-sensitized cell didn't give a high efficiency relative to **PB1**. Hence, the difference in absorption spectra plays a more important role.

The incident photon-to-current conversion efficiency (IPCE) of the DSSCs based on dye **PB4** is measured in the visible region (380–800 nm) in Fig. 7. The IPCE spectrum of **PB4** exhibits a strong absorption in the region of 400–600 nm, and the IPCE reaches 26% at 448 nm and starts to decrease above 650 nm. This is in agreement with the absorption spectrum of dye **PB4** on the TiO_2 film.

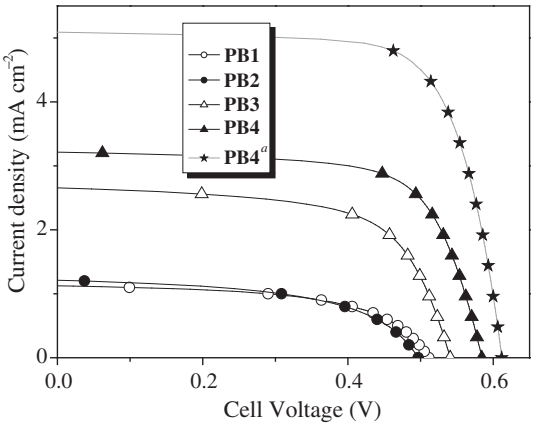

Fig. 6. Typical action spectra of incident photon-to-current conversion efficiencies (IPCE) obtained for nanocrystalline TiO_2 solar cells sensitized by **PB4**.

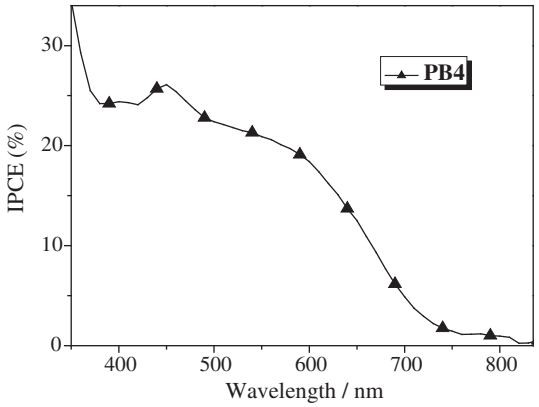

Fig. 7. Photocurrent–voltage characteristics of representative TiO_2 electrodes sensitized with the dyes **PB1**–**4** under AM 1.5 simulated sunlight (100 mW/cm^2).

Moreover, the best conversion efficiency 2.26% was obtained from the **PB4**-sensitized cell prepared by an optimized fabrication process of DSSCs, which didn't include an optimization to the dye. This implies that the efficiency could be further improved.

4. Conclusions

A series of new 2-donor, 6-acceptor BODIPY dyes (**PB1**–**4**) have been synthesized for DSSCs. The photovoltaic behavior of the dye-sensitized cells has been measured. Combination of spectral and electrochemical properties has demonstrated several factors influencing the photovoltaic performance of DSSCs. The structure–property relationship shows that the strong donating power of the donor and better conjugation of π-bridge are favorable for improving the efficiency of DSSCs. Among these dyes, **PB4** with the donor modified by methoxy groups and BODIPY-thiophene as the conjugated bridge reveals strong donating power for the donor and a broader absorption band. The **PB4**-sensitized cell gave the best properties of DSSCs, and the highest photo-to-electron conversion efficiency of 2.26%. This molecular design of 2,6-substituted BODIPY dye has offered a useful approach for development of more efficient DSSCs based on BODIPY derivatives and further improvement of the performance of BODIPY-based DSSCs is in progress.

Acknowledgment

This work was supported by the National Natural Science Foundation of China (Grant Nos. 30870581, 20972149).

References

[1] O'Regan B, Grätzel M. A low-cost, high-efficiency solar cell based on dye-sensitized colloidal TiO_2 films. Nature 1991;353:737–40.
[2] Hagfeldt A, Grätzel M. Molecular photovoltaics. Acc Chem Res 2000;33:269–77.
[3] Grätzel M. Recent advances in sensitized mesoscopic solar cells. Acc Chem Res 2009;42:1788–98.
[4] Yum JH, Walter P, Huber S, Rentsch D, Geiger T, Nüesch F, et al. Efficient far red sensitization of nanocrystalline TiO_2 films by an unsymmetrical squaraine dye. J Am Chem Soc 2007;129:10320–1.
[5] Grätzel M. Conversion of sunlight to electric power by nanocrystalline dye-sensitized solar cells. J Photochem Photobiol A 2004;164:3–14.
[6] Nazeeruddin MK, Kay A, Rodicio I, Humphry-Baker R, Müller E, Liska P, et al. Conversion of light to electricity by cis-X2bis(2,2′-bipyridyl-4,4′-dicarboxylate) ruthenium(II) charge-transfer sensitizers (X = Cl–, Br–, I–, CN– and SCN–) on nanocrystalline TiO_2 electrodes. J Am Chem Soc 1993;115:6382–90.
[7] Nazeeruddin MK, Péchy P, Renouard T, Zakeeruddin SM, Humphry-Baker R, Comte P, et al. Engineering of efficient panchromatic sensitizers for nanocrystalline TiO_2-based solar cells. J Am Chem Soc 2001;123:1613–24.

[8] Imahori H, Umeyama T, Ito S. Large π-aromatic molecules as potential sensitizers for highly efficient dye-sensitized solar cells. Acc Chem Res 2009; 42:1809–18.
[9] Lu HP, Tsai CY, Yen WN, Hsieh CP, Lee CW, Yeh CY, et al. Control of dye aggregation and electron injection for highly efficient porphyrin sensitizers adsorbed on semiconductor films with varying ratios of coadsorbate. J Phys Chem C 2009;113:20990–7.
[10] Imahori H, Matsubara Y, Iijima H, Umeyama T, Matano Y, Ito S, et al. Effects of meso-diarylamino group of porphyrins as sensitizers in dye-sensitized solar cells on optical, electrochemical, and photovoltaic properties. J Phys Chem C 2010;114:10656–65.
[11] Mai CL, Huang WK, Lu HP, Lee CW, Chiu CL, Liang YR, et al. Synthesis and characterization of diporphyrin sensitizers for dye-sensitized solar cells. Chem Commun 2010;46:809–11.
[12] Lee CY, Hupp JT. Dye sensitized solar cells: TiO_2 sensitization with a BODIPY-porphyrin antenna system. Langmuir 2010;26:3760–5.
[13] Edvinsson T, Li C, Pschirer N, Schöneboom J, Eickmeyer F, Sens R, et al. Intramolecular charge-transfer tuning of perylenes: spectroscopic features and performance in dye-sensitized solar cells. J Phys Chem C 2007;111:15137–40.
[14] Wang ZS, Huang CH, Li FY, Weng SF, Ibrahim K, Liu FQ. Alternative self-assembled films of metal-ion-bridged 3,4,9,10-perylenetetracarboxylic acid on nanostructured TiO_2 electrodes and their photoelectrochemical properties. J Phys Chem B 2001;105:4230–4.
[15] Li C, Yum JH, Moon SJ, Herrmann A, Eickemeyer F, Pschirer NG, et al. An improved perylene sensitizer for solar cell applications. ChemSusChem 2008;1:615–8.
[16] Eu S, Katoh T, Umeyama T, Matano Y, Imahori H. Synthesis of sterically hindered phthalocyanines and their applications to dye-sensitized solar cells. Dalton Trans; 2008:5476–83.
[17] Xu W, Peng B, Chen J, Liang M, Cai F. New triphenylamine-based dyes for dyesensitized solar cells. J Phys Chem C 2008;112:874–80.
[18] Ning Z, Zhang Q, Wu WJ, Pei HC, Liu B, Tian H. Starburst triarylamine based dyes for efficient dye-sensitized solar cells. J Org Chem 2008;73:3791–7.
[19] Li G, Jiang KJ, Li YF, Li SL, Yang LM. Efficient structural modification of triphenylamine-based organic dyes for dye-sensitized solar cells. J Phys Chem C 2008;112:11591–9.
[20] He JX, Wu WJ, Hua JL, Jiang YH, Qu SY, Li J, et al. Bithiazole-bridged dyes for dye-sensitized solar cells with high open circuit. J Mater Chem 2011;21: 6054–62.
[21] Ma XM, Hua JL, Wu WJ, Jin YH, Meng FS, Zhan WH, et al. A high-efficiency cyanine dye for dye-sensitized solar cells. Tetrahedron 2008;64:345–50.
[22] Wu WJ, Hua JL, Jin YH, Zhan WH, Tian H. Photovoltaic properties of three new cyanine dyes for dye-sensitized solar cells. Photochem Photobiol Sci 2008;7:63–8.
[23] Hara K, Tachibana Y, Ohga Y, Shinpo A, Suga S, Sayama K, et al. Dye-sensitized nanocrystalline TiO_2 solar cells based on novel coumarin dyes. Sol Energ Mat Sol C 2003;77:89–103.
[24] Hara K, Sato T, Katoh R, Furube A, Ohga Y, Shinpo A, et al. Molecular design of coumarin dyes for efficient dye-sensitized solar cells. J Phys Chem B 2003; 107:597–606.
[25] Hara K, Wang ZS, Sato T, Furube A, Katoh R, Sugihara H, et al. Oligothiophene-containing coumarin dyes for efficient dye-sensitized solar cells. J Phys Chem B 2005;109:15476–82.
[26] Wang ZS, Cui Y, Hara K, Dan-oh Y, Kasada C, Shinpo A. A high-light-harvesting-efficiency coumarin dye for stable dye-sensitized solar cells. Adv Mater 2007;19:1138–41.
[27] Seo KD, Song HM, Lee MJ, Pastore M, Anselmi C, Angelis FD, et al. Coumarin dyes containing low-band-gap chromophores for dye-sensitised solar cells. Dyes Pigm 2011;90:304–10.
[28] Wang ZS, Li FY, Huang CH, Wang L, Wei M, Jin LP, et al. Photoelectric conversion properties of nanocrystalline TiO_2 electrodes sensitized with hemicyanine derivatives. J Phys Chem B 2000;104:9676–82.
[29] Chen YS, Li C, Zeng ZH, Wang WB, Wang XS, Zhang BW. Efficient electron injection due to a special adsorbing group's combination of carboxyl and hydroxyl: dye-sensitized solar cells based on new hemicyanine dyes. J Mater Chem 2005;15:1654–61.
[30] Horiuchi T, Miura H, Sumioka K, Uchida S. High efficiency of dye-sensitized solar cells based on metal-free indoline dyes. J Am Chem Soc 2004;126: 12218–9.
[31] Kuang D, Uchida S, Humphry-Baker R, Zakeeruddin SM, Grätzel M. Organic dye-sensitized ionic liquid based solar cells: remarkable enhancement in performance through molecular design of indoline sensitizers. Angew Chem Int Ed 2008;47:1923–7.
[32] Ito S, Miura H, Uchida S, Takata M, Sumioka K, Liska P, et al. High-conversion-efficiency organic dye-sensitized solar cells with a novel indoline dye. Chem Commun 2008;5194–6.
[33] Chen RK, Yang XC, Tian HN, Wang XN, Hagfeldt A, Sun LC. Effect of tetrahydroquinoline dyes structure on the performance of organic dye-sensitized solar cells. Chem Mater 2007;19:4007–15.
[34] Hao Y, Yang XC, Cong JY, Tian HN, Hagfeldt A, Sun LC. Efficient near infrared D–π–A sensitizers with lateral anchoring group for dye-sensitized solar cells. Chem Commun 2009;4031–3.
[35] Tian HN, Yang XC, Chen RK, Pan YZ, Li L, Hagfeldt A, et al. Phenothiazine derivatives for efficient organic dye-sensitized solar cells. Chem Commun 2007;3741–3.
[36] Loudet A, Burgess K. BODIPY dyes and their derivatives: syntheses and spectroscopic properties. Chem Rev 2007;107:4891–932.
[37] Ziessel R, Ulrich G, Harriman A. The chemistry of BODIPY: a new *El Dorado* for fluorescence tools. New J Chem 2007;31:496–501.
[38] Ulrich G, Ziessel R, Harriman A. The chemistry of fluorescent BODIPY dyes: versatility unsurpassed. Angew Chem Int Ed 2008;47:1184–201.
[39] Boens N, Qin WW, Baruah M, Borggraeve WMD, Filarowski A, Smisdom N, et al. Rational design, synthesis, and spectroscopic and photophysical properties of a visible-light-excitable, ratiometric, fluorescent near-neutral pH indicator based on BODIPY. Chem Eur J 2011;17:10924–34.
[40] Yin SC, Leen V, Snick SV, Boens N, Dehaen W. A highly sensitive, selective, colorimetric and near-infrared fluorescent turn-on chemosensor for Cu^{2+} based on BODIPY. Chem Commun 2010;46:6329–31.
[41] Qin WW, Baruah M, Sliwa M, Auweraer MVD, Borggraeve WMD, Belionne D, et al. Ratiometric, fluorescent BODIPY dye with aza crown ether functionality: synthesis, solvatochromism, and metal ion complex formation. J Phys Chem A 2008;112:6104–14.
[42] Hattori S, Ohkubo K, Nagano T, Lemmetyinen H, Fukuzumi S. Charge separation in a nonfluorescent donor-acceptor dyad derived from boron dipyrromethene dye, leading to photocurrent generation. J Phys Chem B 2005;109: 15368–75.
[43] Erten-Ela S, Yilmaz MD, Icli B, Dede Y, Icli S, Akkaya EU. A panchromatic boradiazaindacene (BODIPY) sensitizer for dye-sensitized solar cells. Org Lett 2008;10:3299–302.
[44] Rousseau T, Cravino A, Bura T, Ulrich G, Ziessel R, Roncali J. BODIPY derivatives as donor materials for bulk heterojunction solar cells. Chem Commun 2009;1673–5.
[45] Rousseau T, Cravino A, Bura T, Ulrich G, Ziessel R, Roncali J. Multi-donor molecular bulk heterojunction solar cells: improving conversion efficiency by synergistic dye combinations. J Mater Chem 2009;19:2298–300.
[46] Forgie JC, Skabara PJ, Stibor I, Vilela F, Vobecka Z. New redox stable low band gap conjugated polymer based on an EDOT-BODIPY-EDOT repeat unit. Chem Mater 2009;21:1784–6.
[47] Kumaresan D, Thummel RP, Bura T, Ulrich G, Ziessel R. Color tuning in new metal-free organic sensitizers (Bodipys) for dye-sensitized solar cells. Chem Eur J 2009;15:6335–9.
[48] Kolemen S, Cakmak Y, Erten-Ela S, Altay Y, Brendel J, Thelakkat M, et al. Solid-state dye-sensitized solar cells using red and near-IR absorbing BODIPY sensitizers. Org Lett 2010;12:3812–5.
[49] Kolemen S, Bozdemir OA, Cakmak Y, Barin G, Erten-Ela S, Marszalek M, et al. Optimization of distyryl-BODIPY chromophores for efficient panchromatic sensitization in dye sensitized solar cells. Chem Sci 2011;2:949–54.
[50] Wang JB, Fang XQ, Pan X, Dai SY, Song QH. New 2,6-modified BODIPY sensitizers for dye-sensitized solar cells. Chem Asian J, doi:10.1002/asia.201100779.
[51] Siska WN, Onob N, Yanob T, Wadab M. Photostability studies of three new bicyclo-boron dipyrromethene difluoride dyes. Dyes Pigm 2002;55:143–50.
[52] Jiao LJ, Yu CJ, Li JL, Wang ZY, Wu M, Hao E. β-formyl-BODIPYs from the Vilsmeier–Haack reaction. J Org Chem 2009;74:7525–8.
[53] Bonardi L, Ulrich G, Ziessel R. Tailoring the properties of boron-dipyrromethene dyes with acetylenic functions at the 2,6,8 and 4-B substitution positions. Org Lett 2008;10:2183–6.
[54] Zhang CN, Huo ZP, Huang Y, Dai SY, Wang M, Tang YT, et al. Electrolyte effects on photoelectron injection and recombination dynamics in dye-sensitized solar cells. J Photochem Photobiol A 2010;213:87–92.
[55] Steck EA, Day AR. Reactions of phenanthraquinone and retenequinone with aldehydes and ammonium acetate in acetic acid solution. J Am Chem Soc 1943;65:452–6.
[56] Thomas KRJ, Hsu YC, Lin JT, Lee KM, Ho KC, Lai CH, et al. Chem Mater 2008;20: 1830–40.